Research note

Effect of Mixer Rotational Speed on Heat Transfer Coefficient in Preparation of Nickle Perovskite From Laboratory to Bench Scale

A. Ebrahimi, M. Bandari and M. Parvari[*]

School of Chemical Engineering, Iran University of Science and Technology

Abstract
In this study, we examined a scale-up to production of nickel perovskite catalyst, used in the conversion of natural gas to synthesis gas, using the sol-gel method in the laboratory and a bench-scale reactor. The required volume of solvent and catalyst activity in the methane-reforming reaction was determined from the optimum catalyst production conditions at the laboratory scale. This information was then used to design the bench-scale unit. We used heat-transfer models in a non-continuous bench reactor and scale-up fundamentals to achieve the same physical and chemical properties of the catalyst as that in the laboratory sample. A correlation coefficient corresponding to the experiment conditions, including the stirrer geometry, is presented based on the heat transfer equations in stirred tanks. This correlation can be used to estimate the heat-transfer coefficient at larger scales, such as in a pilot reactor.

Keywords: *Scale-up, Perovskite, Reforming, Sol-Gel*

1- Introduction

Scale up is inherent in all industrial activity. Scale up is the process or group of activities by which one moves from the calculation, studies, and demonstration to a successful commercial operation facility. Scaling up of a mixer requires an understanding of some of the basic principles of fluid mixing and their roles in determining process performance. In scale up we must have geometric and dynamic similarity. Geometric similarity means that the laboratory and bench scale must be similar in dimensions. Also, in dynamic similarity the ratio of inertia forces of both scales must the equal to ratio of viscous forces, ratio of gravitational forces and the surface forces.

$$\frac{(F_I)_M}{(F_I)_P} = \frac{(F_V)_M}{(F_V)_P} = \frac{(F_G)_M}{(F_G)_P} = \frac{(F_I)_M}{(F_G)_P} \qquad (1)$$

Dimensionless groups relating fluid forces are:

$$\frac{F_I}{F_v} = \mathrm{Re} = \frac{ND^2 p}{\mu} \qquad (2)$$

---
[*] Corresponding author: parvari@iust.ac.ir

$$\frac{F_i}{F_g} = Fr = \frac{N^2 D}{g} \qquad (3)$$

$$\frac{F_i}{F_\sigma} = We = \frac{N^2 D^3 p}{\sigma} \qquad (4)$$

Laboratory studies are essential when the production of a chemical is considered for the first time. This includes feasibility studies of a process that minimize the losses caused by the effects of unknown parameters. To investigate such parameters and determine the optimum method of achieving a reliable industrial design, it is essential to undertake process studies in the laboratory as well as bench, pilot, and industrial units. Generally, chemical reactions and reactors are important, and the factors that affect the reaction must be studied at several stages. These factors include heat transfer phenomena in mixed reactors. Many different equations for estimating h, the convective heat transfer coefficient, in stirred tanks have been presented for different mixers. The following equations are presented for a three-blade turbine mixer with a thermal jacket heating system [1]:

$$\frac{hD_T}{K} = 0.37(\text{Re})^{0.67}(\text{Pr})^{0.33}(\frac{\mu}{\mu_w})^{0.14} \qquad (5)$$

$$\text{Pr} = \frac{\mu.C_P}{K} \ , \ \text{Re} = \frac{\rho N D_a^2}{\mu} \qquad (6)$$

The sol-gel process is a technique for producing ceramics and porous material at low temperatures. This technique has advantages (e.g., low reaction temperature) that make it useful in the preparation of catalysts. In this method, a solution of primary salts converts to gelatin through a batch distillation process. The desired catalysts will then form via thermal operations. Sol-gel operations are generally performed in one of two ways: a colloidal method in which colloidal particles are dispersed in solvent and then converted to gel; and a method in which organic–metallic compounds such as alcoxides polymerize in solvent to form a network gel.

The production of perovskite catalysts is one of the applications of the sol-gel method. These catalysts can be used for converting natural gas to syngas. Three general processes are used to convert natural gas to syngas: steam reforming, partial oxidation of methane, and carbon dioxide reforming. The main difference among these processes is the ratio of hydrogen to carbon monoxide in the resulting gas. The choice of process depends on the intended use of the syngas. The convenient choice for the hydrogenation process is steam reforming, in which the ratio of hydrogen to carbon monoxide is high ($H_2/CO = 3$). In contrast, a lower ratio of H_2 to CO is appropriate for reactions where hydrogen and carbon monoxide react, such as methanol and Fischer–Tropsch synthesis [6, 7].

The catalysts used for converting natural gas to syngas can be divided into two groups: those with a noble metal as the main element [8-15], and compounds with an iron-group metal such as Fe, Co, or Ni as the main element. Nickel is the most active metal in this group and is useful in the conversion of natural gas to syngas. Nickel has been used in several catalysts, such as inorganic-supported catalysts and perovskites [16-18].

The use of La(Ni,Al)O$_3$ solid solution can be effective in the dry reforming of methane for syngas production [19].

In the present work, we study the heat transfer effects and scale-up method of a reactor for the preparation of nickel perovskite catalyst via the sol-gel method. This is studied from laboratory to pilot-scales.

2- Experimental

2.1- Apparatus

The laboratory-scale system included a 500-cm^3 glass balloon as a reactor, equipped with a thermocouple and a glass condenser for collecting solvent vapors leaving the reactor. A 1-kW electrical heating system was used to provide the required reaction temperature. Mixing in the reactor is performed using a magnetic mixer.

The capacity of the bench reactor was determined for the production of 1 kg of perovskite catalyst in each batch. The bench reactor was a cylindrical tank of 29 cm in ID and 34 cm in height, equipped with a condenser for collecting solvent vapors, two feed entrances, two thermocouples for measuring the temperature of the fluid inside the reactor and the tank wall, eight baffles to prevent vortex, and a two-blade turbine mixer. The total volume of reactant fluids was 10 l. A 2-kW heating system fitted as an electrical jacket was used to warm the reactor contents. Fig. 1 shows a schematic diagram of the reactor system.
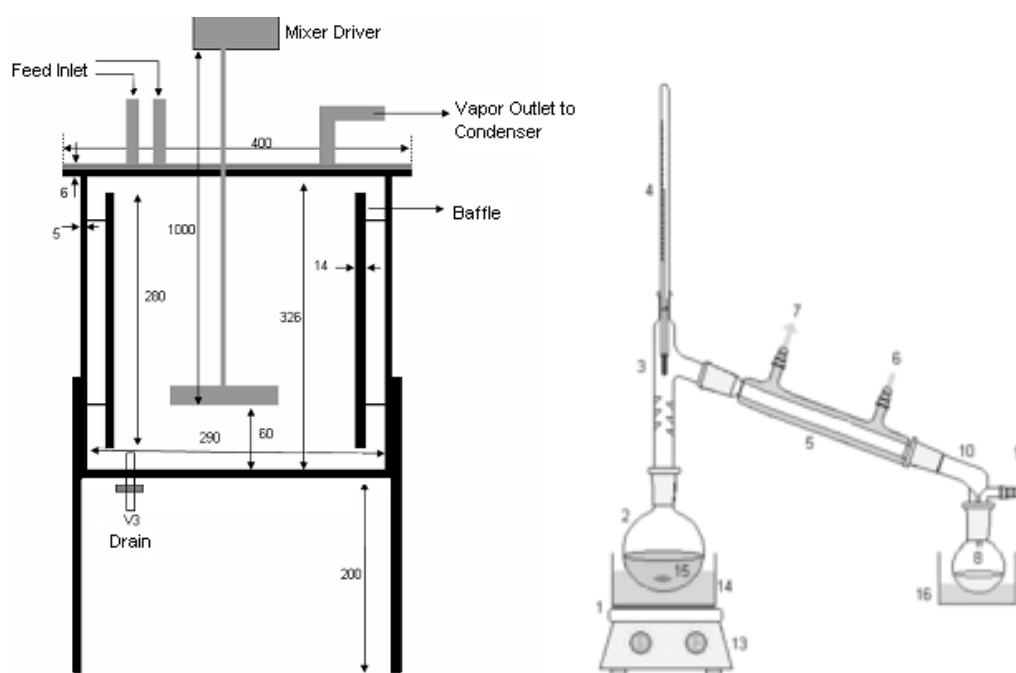
Figure 1: Schematic Diagram of a) Bench Reactor Setup (All dimensions are in mm) b) Lab scale set up 1: Heat source 2: Still pot 3: Still head 4: Thermometer/Boiling point temperature 5: Condenser 6: Cooling water in 7: Cooling water out 8: Distillate/receiving flask 9: Vacuum/gas inlet 10: Still receiver 11: Heat control 12: Stirrer speed control 13: Stirrer/heat plate 14: Heating bath 15: Stirrer bar 16: Cooling bath

2.2- Experiments

We first used experimental results to determine the minimum required volumes of solvent to dissolve the primary salts containing nickel, aluminum, and lanthanum nitrates. Precursor solutions corresponding to each of the elements were prepared by dissolving the salts in propionic acid in the following manner. The required amount of solvent was determined and the salts were then dissolved separately in the optimum amount of propionic acid on a heating system. The formation of precursor solutions took about 15–20 min. The primary solutions were then mixed together. The final gel was obtained by differential distillation of the resulting mixture for about 4 h. The desired catalyst was formed by calcinations of the gel in an electrical furnace.

We measured the convective heat transfer coefficient inside the tank (*h*) and during sol-gel process bench plant experiments to study the system performance. The objectives of the bench reactor experiments were to investigate the effect of mixer rotation on heat transfer and to formulate a model for determining the convective heat transfer coefficient for the inside of the tank. According to the differences in modeling the system before and after boiling, the experiments were performed in two parts and at mixer rotations of 60, 90, 120, 150, 170, and 230 rpm for water and the final catalyst

solution.

In the experiments before boiling, the temperature of the fluid was recorded several times at fixed mixer rotation and thermal power. After a specified increase in temperature, temperatures were recorded at three points in the solution and also at the tank wall. Using this information, *h* was obtained at each step of the temperature increase. The experiments after boiling were started once condensation had formed in the condenser. After every 10-min period, we recorded the temperature of the solution at three points in the fluid, the temperature of the tank shell, and the volume of condensed water. Using this information, the heat transfer coefficient was calculated for each period. The experiments were performed for water and the final catalyst preparation solution.

3- Results and discussion

3.1- Experimental results

The amount of solvent required to prepare precursor solutions was determined from the results obtained in the laboratory studies. This amount is very important, as shown in Table 1. The optimum temperature for the differential distillation process was 160°C. Following formation of the gel, the required temperature and time of calcination was 750°C and 4 h, respectively.

Table 1. Solubility of the starting salts in propionic acid

Salt name	Amount of salt	Amount of solvent required
Lanthanum nitrate	1 g	2 cc
Aluminum nitrate	1 g	1.6 cc
Nickel nitrate	1 g	2.1 cc

3.2- Bench reactor design

The most important parameter in designing a stirred tank reactor is the volume, which is dependent on the volume of precursor solutions. Using laboratory data, the amounts of reactants required to produce 1 kg of catalyst are as follows:

1) Nickel nitrate	390	g
2) Aluminum nitrate	1170	g
3) Lanthanum nitrate	1940	g

The amount of solvent required to prepare the solution of the above salts is equal to:

1) Nickel nitrate	820	cc
2) Aluminum nitrate	1880	cc
3) Lanthanum nitrate	3880	cc

Therefore, the total volume of the reactor is 6.58 l. Taking into account an amount of void volume at the top of the solution for separating the vapor phase and enabling discharge through the condenser, the total volume of the tank is considered to be 10 l. In order to fix the reaction temperature, an electrical thermal jacket was used as a heating system. Thermal power calculations were undertaken in two parts:

a) The thermal power required to increase the solution temperature to the reaction temperature (160°C) in 30min, $Q = 1.56$ kW.

b) The thermal power required to fix the temperature during the reaction, which compensates losses and provides the latent heat of the vaporization of the solution. After calculation, we have:

$$Q_{loss} = 0.045 \quad \text{kW} \tag{7}$$

$$Q_{latentheat} = 0.331 \quad \text{kW} \tag{8}$$

Accordingly, a 2-kW heating system with potentiometer and wattmeter was used to regulate the solution temperature. To recover the solvents leaving the reactor, a double-pipe condenser was used with the following characteristics:

Shell ID	=	3 in
Tube ID	=	0.75 in
Exchanger length	=	0.5 m

To provide mixing, we used a two-blade mixer with the following characteristics:
l = 5 cm, b = 2.5 cm, Z = 6 cm, D_a = 11 cm

The electrical motor of the mixer has the characteristics: output power = 27 W, maximum moment = 400 N.cm at 40 rpm, and velocity range = 40–200 rpm.

3.3- Results in the bench reactor

In this section, we present calculations for water at 60 rpm mixer rotation as an example. As previously stated, the observations are performed at two stages: before and after boiling. It was assumed that the heating rate used to increase the temperature of the solution to boiling point was equal to the convective heat transfer between the tank wall and the solution. In this case, we have:

$$Q_1 = mc_p\Delta T_1 \tag{9}$$

$$Q_2 = hA\Delta T_2 \tag{10}$$

$$Q_1 = Q_2 \tag{11}$$

The heat transfer area was assumed to be equal to the wetted surface, which is constant here. Assuming that the density and specific heat capacity of water are 1000 kg/m^3 and 4.21 kJ/kg°C, respectively, and that the reactor volume is 0.01 m^3, we have:

$Q_1 = mc_p \Delta T_1 = \rho V c_p \Delta T_1 = 1000 \ W$ ********

In this case, only 1 of the 2 kW provided by the heater is consumed for heating the water. The remaining heat is consumed by the warming of the tank wall, heat transfer with the void space in the tank, and heat losses. Therefore, we can write:

$$Q_2 = Q_1 = hA\Delta T_2 \qquad (12)$$

$$A = \pi D_T L \qquad (13)$$

$$1000 = h(0.13659)\Delta T_2 \qquad (14)********$$

Consequently: $\quad h = \dfrac{7319.14}{\Delta T_2} \qquad (15)$

Because of the difference in ΔT_2 for each period, there is a different heat transfer coefficient for each period. For example, if

$\Delta T_2 = 11°C$, we have:

$$h = 665.36 \ \frac{W}{m^2 °C} \ ******$$

Other values of h for this and other periods, for the two fluids of water and catalyst precursor solution, are presented in Tables 2 and 3. We plotted changes in water temperature over time, in which the slope of the temperature profile curve represents the effect of mixer rotation on heat transfer. An example of such a plot at 60 rpm mixer rotation for water is shown in Fig. 2. Other cases are compared in Fig. 3. According to the h values presented in Tables 2 and 3, it is clear that h increases with increasing mixer speed. In addition, an increase in the slope of the temperature profile curve indicates the effect of mixer speed on the heat transfer rate and the rate of temperature increase of the fluid inside the reactor.

Table 2. Heat convection coefficient (W/m^2°C) for water at different mixer speeds

Solution temperature (ºC)	60 rpm	90rpm	120rpm	150rpm	170rpm	230rpm
80	665	601	690	878	896	947
90	2033	1654	2206	3346	3979	4795
96	1829	2206	2877	2342	2558	2996
Average	1509	1487	1924	2189	2477	2912

Table 3. Heat convection coefficient (W/m2°C) for precursor solution at different mixer speeds

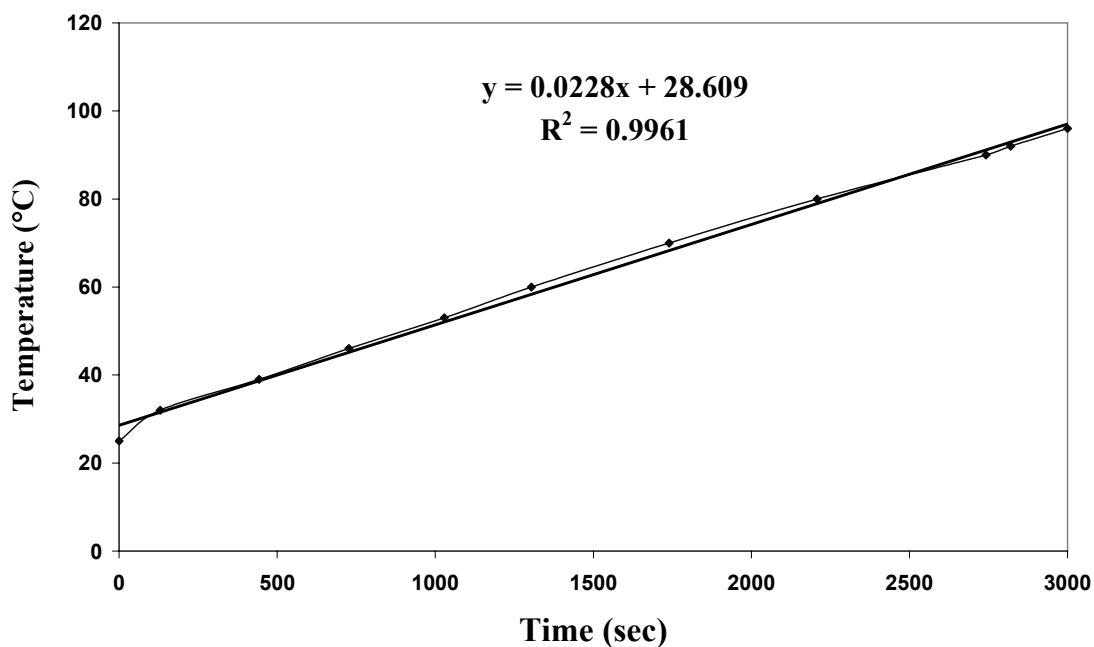| Solution temperature (ºC)	60 rpm	90rpm	120rpm	150rpm	170rpm	230rpm
80	475	428	492	587	491	688
90	570	668	703	838	843	725
96	633	750	985	903	1073	838
Average	560	615	727	776	802	750

$$y = 0.0228x + 28.609$$
$$R^2 = 0.9961$$

Figure 2. Temperature profile for water at 60 rpm mixing
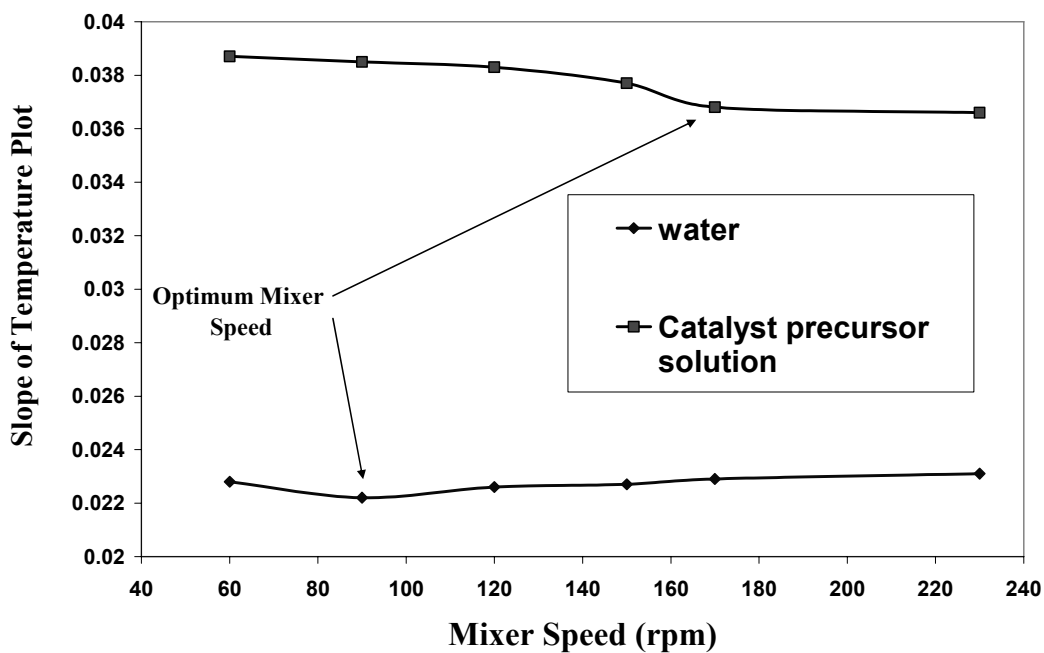
Figure 3. The slops of temperature plot versus mixer speed for water and catalyst precursor solution

Fig. 3 shows that the slope at 60 rpm is greater than that at other speeds. This means that the heat transfer coefficient is greatest at 60 rpm. However, this observation is contrary to the results of previous studies that report that *h* increases with increased mixing. This discrepancy may reflect inadequate mixing. In other words, a rotation of 60 rpm fails to adequately mix the solution; consequently, the thermocouple position beside the wall results in a higher measured temperature than that of the solution. Thus, measured temperature differences between the wall and fluid are underestimated, leading to artificially high *h* values. Other rotation speeds provide adequate mixing and satisfactory results. Similar problems occur for the precursor solution at 60 to 170 rpm. Therefore, the appropriate rotation is 230 rpm for this case and 90 rpm for water. It is important to investigate why low rates of

rotation produce good mixing in water but poor mixing in the catalyst precursor solution. The Prandtl number for water and the catalyst precursor solution, which is the ratio of viscous force to heat conduction, is equal to 1.643 and 10.245 respectively. A lower Prandtl number indicates higher thermal conductivity. Thus, there is high heat transfer in water at 90 rpm despite the poor mixing. However, this is not the case for catalyst precursor solution, so 230 rpm rotation has been selected to provide adequate mixing. In the following, the experimental values of h are compared with calculated values from the heat transfer equation (Eq. 1) for a stirred tank and a three-blade turbine mixer. This equation is selected because of the geometric similarity of a three-blade mixer to the mixer used in the experiments. Related values are compared in Figs. 4 and 5.
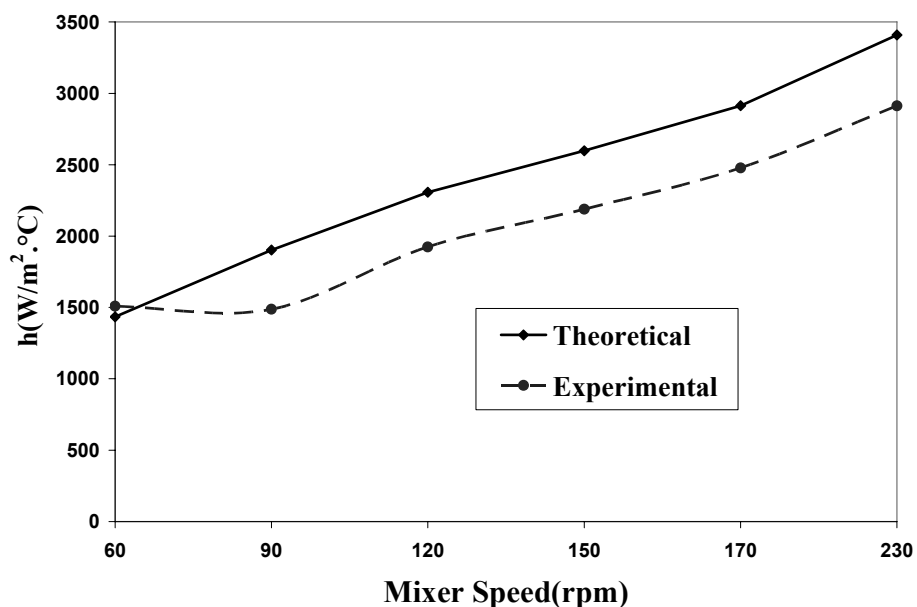

Figure 4. Comparison of theoretical and experimental heat transfer coefficients for water
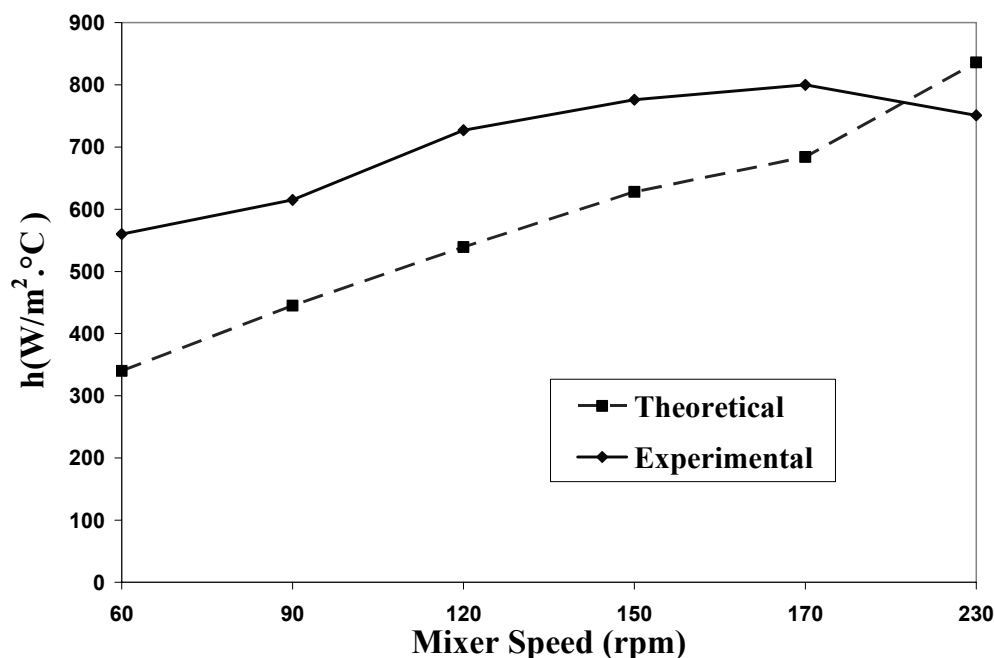
Figure 5. Comparison of theoretical and experimental heat transfer coefficients for catalyst precursor solution

Fig. 4 shows that experimentally obtained values of *h* are smaller than those determined for the three-blade mixer, which reflects the difference in the numbers of blades. The rotation speed of 60 rpm is an exception to this trend, reflecting inadequate mixing. It is clear from the figure that the optimum mixer rotation for water is 90 rpm, as the results are consistent above this rate.

According to Fig. 5, for a catalyst precursor solution at up to 170 rpm mixing, experimental values of *h* are greater than theoretical ones, again reflecting inadequate mixing. However, at 230 rpm the result is satisfactory. Therefore, 230 rpm is considered to be optimum for catalyst precursor solution. The corresponding Reynolds number is used for a scale-up based on kinematic similarity. The figure indicates that the difference between the experimental and theoretical data decreases

as the mixer rotation increases to 230 rpm. In the following, a correlation for the convective heat transfer coefficient, similar to the one used for the three-blade mixer, is presented based on the experimental data. The general form of these equations for turbine mixers is as follows:

$$\frac{hD_T}{k} = a(\text{Re})^{0.67}(\text{Pr})^{0.33}\left(\frac{\mu}{\mu_w}\right)^{0.14} \qquad (16)$$

The powers of the Reynolds and Prandtl numbers, as well as the viscosity correction factor, are almost constant for most cases. The most influential factor in the above equation is "*a*", which indicates the effect of mixer geometry on the heat transfer coefficient. For a three-blade turbine mixer, *a* is equal to 0.37. We conducted a regression analysis of the experimental data to

determine the value of *a* for each mixer, to present a correlation coefficient for scale-up, and to obtain a heat transfer coefficient for larger reactors. The regression analysis uses data measured from water. Thus, the Prandtl number and viscosity correction factor are constant, and the effective variable parameter is the Reynolds number, which varies with mixer rotation. After simplification, the equation reduces to:

$$M = a(\text{Re})^{0.67} \tag{17}$$

Where M is a number obtained for each mixer rotation with the insertion of variables, and is defined as:

$$M = \frac{\left(\dfrac{hD_T}{k}\right)}{(\text{Pr})^{0.33}\left(\dfrac{\mu}{\mu_w}\right)^{0.14}} \tag{18}$$

The data used for the regression and their accuracy are presented in Tables 4 and 5. The regression analysis yields a value of *a* of 0.3022. Thus, the correlation takes the form:

$$M = 0.3022(\text{Re})^{0.67} \tag{19}$$

$$\frac{hD_T}{k} = 0.3022(\text{Re})^{0.67}(\text{Pr})^{0.33}\left(\frac{\mu}{\mu_w}\right)^{0.14} \tag{20}$$

The accuracy of the correlation was tested using data at 120 rpm rotation for water and 230 rpm for catalyst precursor solution. In the stage after boiling, we studied the simultaneous effects of boiling phenomena and convection. The end time of the reaction in the sol-gel process was estimated at each rotation from the amount of collected condensates. Modeling of the system is complex in this stage because of the continuous evaporation of water, a decrease in fluid depth, and a decrease in the heat transfer area. In addition, the temperature difference between the wall and fluid is variable at each time interval, and this must be considered. In these calculations it was assumed that the heat transfer area is equal to the wetted surface, which varies with time. To use the equation, variations in ΔT_2 and A are obtained over time. According to the surface calculation formula, variations in A are directly dependent on height (L), which is easily determined. The equation describing variations in ΔT_2 can be obtained in a similar way. Table 6 shows the calculations for water at 60 rpm.

$$L = (-0.0478t + 15.152) \times 10^{-2} \quad m \tag{21}$$

Table 4. Data used in the regression

	60 rpm	90rpm	150rpm	170rpm	230rpm
Reynolds	45318	67977	113295	128402	173720
M	344.13	500	735.77	832.7	978.73

Table 5. Accuracy of the regression equation

Solution	Mixer speed	h (W/m²°C) Experimental	h (W/m²°C) Calculated from equation regression	% Eror
Water	120 rpm	1924	1885	2.02
Catalyst precursor solution	230 rpm	751	682	9

Table 6. Calculated data for water at 60 rpm mixing

Solution temperature (°C)	Wall temperature (°C)	Volume of Condensate (cc)	Volume of Remained water (cc)	Liquid height (cm)	Time (min)	ΔT Wall & solution	h W/m²°C	h average W/m²°C
-	-	0	10000	15	0	-		
97.3	102.1	300	9700	14.68	10	4.8	1864	
97.4	103.2	640	9360	14.17	20	5.8	1633	
97.3	103.6	940	9060	13.71	30	6.3	1665	1838
97.3	104.4	1240	8760	13.27	40	7.1	1755	
97.3	105.1	1580	8420	12.74	50	7.6	2272	
97.5	105.5	1920	8080	12.24	60	7.9	2292	

$$A = \pi D_T L = 0.009106 \times \left(-0.0478t + 15.152\right) \ m^2 \tag{22}$$

$$\dot{m} = 0.527 \ gr.s^{-1}$$

$$\Delta T = -6 \times 10^{-6} t^4 + 0.0007 t^3 - 0.0309 t^2 + 0.6133t + 1.1 \tag{23}$$

$$Q_{latentheat} = 1191.785 \ W$$

Equating the amount of heat transferred by convection with the heat required for vaporization, we have:

$$1191.785 = h\left(0.009106\right)\left(-0.0478t + 15.152\right)$$
$$\left(-0.000006t^4 + 0.0007t^3 - 0.0309t^2 + 0.6133t + 1.1\right) \tag{24}$$

In this manner, we obtained an equation for calculating the heat transfer coefficient in terms of time (*t*). The heat transfer coefficient can be calculated by substituting values of time at each 10-min period. The calculations for several speeds are presented in Fig. 6. Plots of depth and temperature difference versus time are also presented

(Figs. 7 and 8). Similar experiments were performed without mixing, which provide only the heat transfer coefficient related to boiling.

Comparing the value of *h* before and after boiling, it is clear that the heat transfer coefficient increases markedly during the boiling stage. In this stage, heat transfer due to boiling ($h_{boiling}$) and convection interact. Therefore, values of *h* observed from experiments ($h_{effective}$) represent a combination of these effects. This is well demonstrated in Figures 9 and 10.
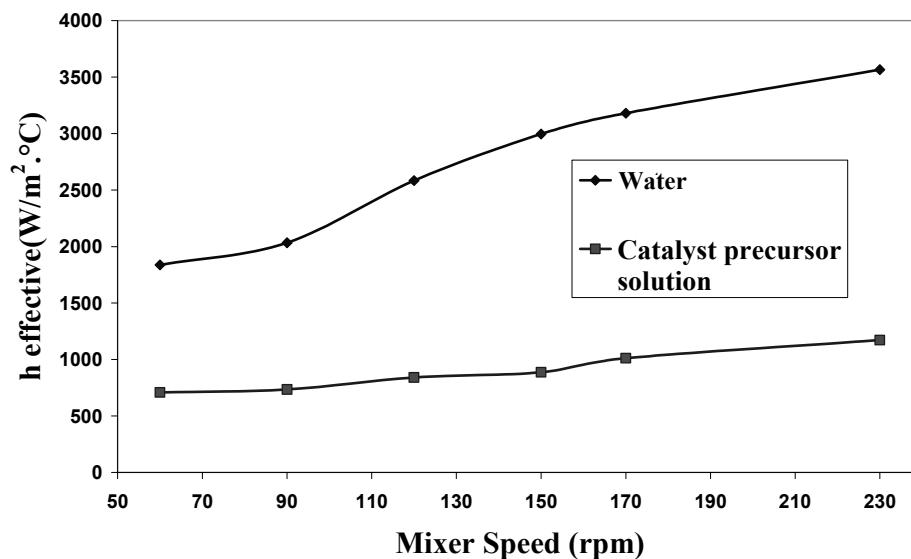
Figure 6. Calculated convective heat transfer coefficients after boiling and for different mixer speeds
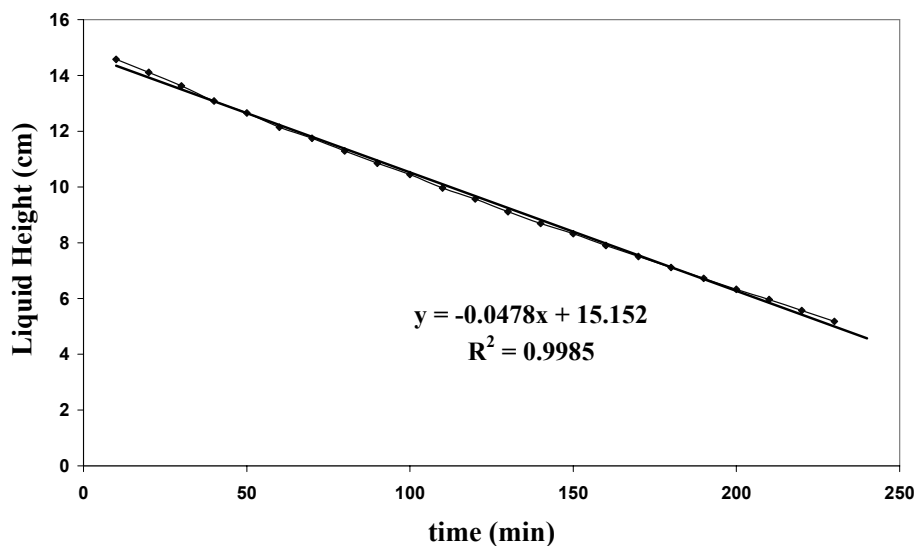
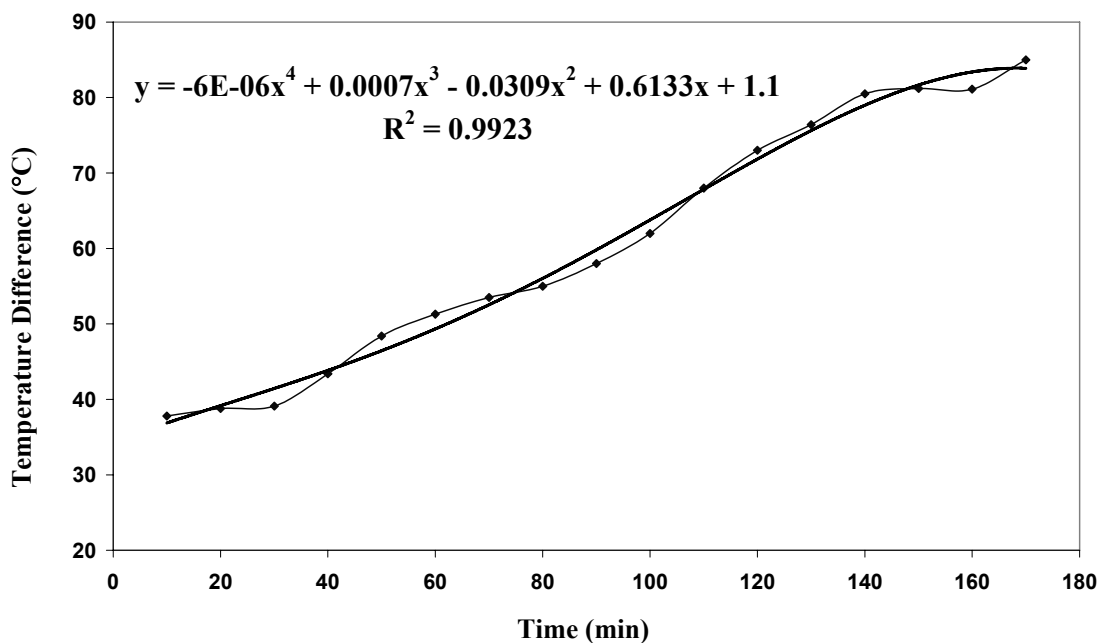**Figure 7.** Plot of liquid height versus time for water

$$y = -6E\text{-}06x^4 + 0.0007x^3 - 0.0309x^2 + 0.6133x + 1.1$$
$$R^2 = 0.9923$$

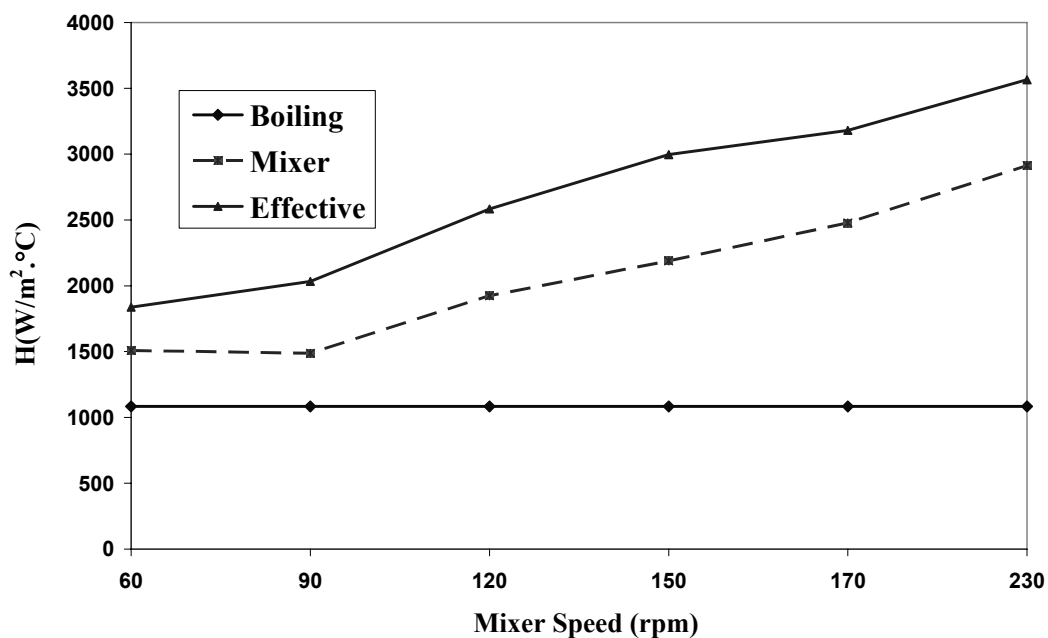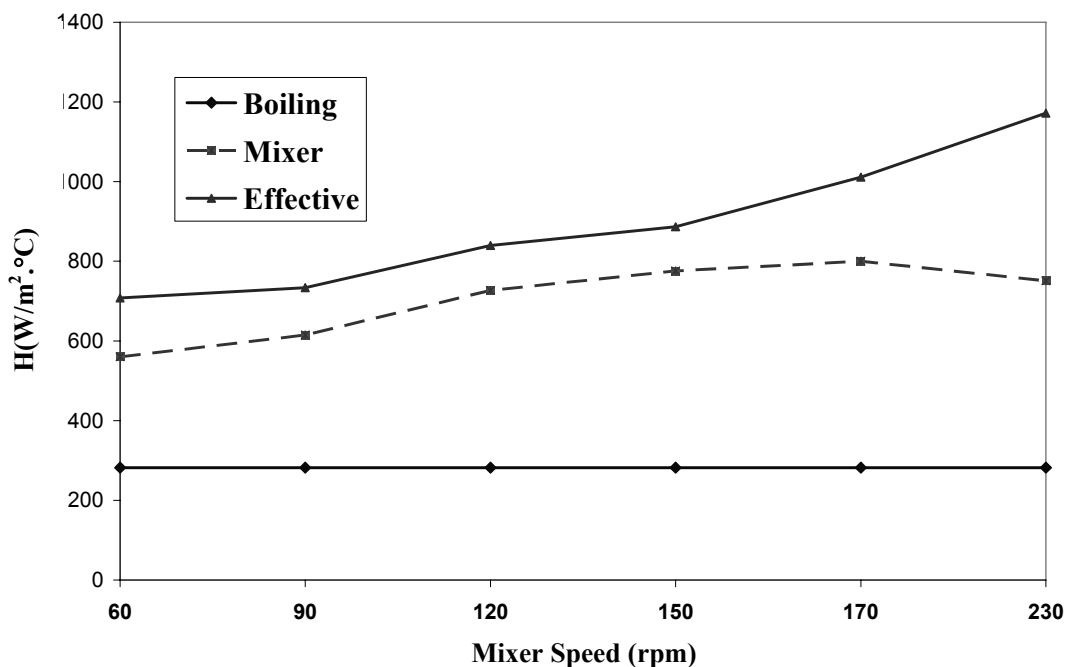**Figure 8.** Plot of temperature difference versus time for water

Figure 9. Interaction between h (boiling) and h (mixer) and compare with h (effective) for water

Figure 10. Interaction between h (boiling) and h (mixer) and compare with h (effective)
for catalyst precursor solution

3.4- Results of catalytic performance in a reactor

To study the performance of the prepared catalysts in a bench reactor and compare the results with those of catalysts prepared at a lab-scale [19], we carried out dry reforming at similar conditions. The results are compared in Figs. 11 and 12, which show methane conversion and hydrogen selectivity, respectively. The performances of the two catalysts prepared at different scales are similar, indicating that the accuracy of the calculations and the design of the bench unit are reliable. Thus, scale-up calculations up to a pilot plant can be performed based on the above results.

4. Conclusions

According to the experiment results, an increase in mixer rotation produces a related increase in the amount of transferred heat. The optimum rotation of the mixer required to ensure adequate mixing is 90 rpm for water and 230 rpm for the catalyst precursor solution. Using experimental results from a bench unit, we determined a correlation for estimating *h* in the form of Equation (20) within a stirred tank for a two-blade turbine mixer. This correlation can be used for estimating the convective heat transfer coefficient within reactors at larger scales.
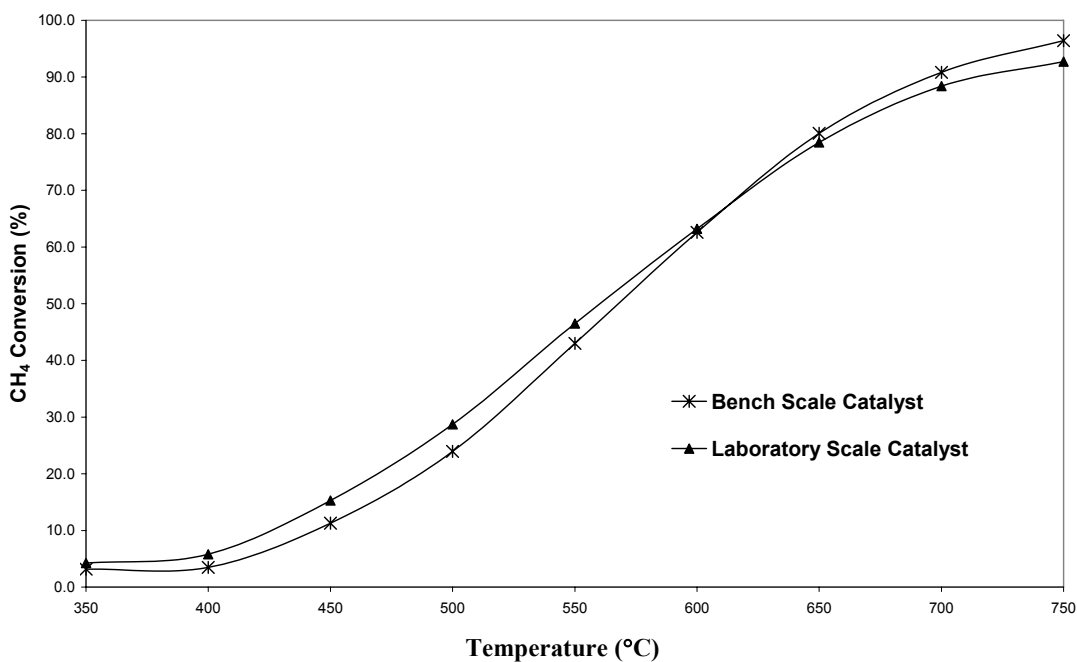
Figure 11. Comparison of methane conversion in a dry reforming reaction using catalysts prepared at the laboratory- and bench-scales
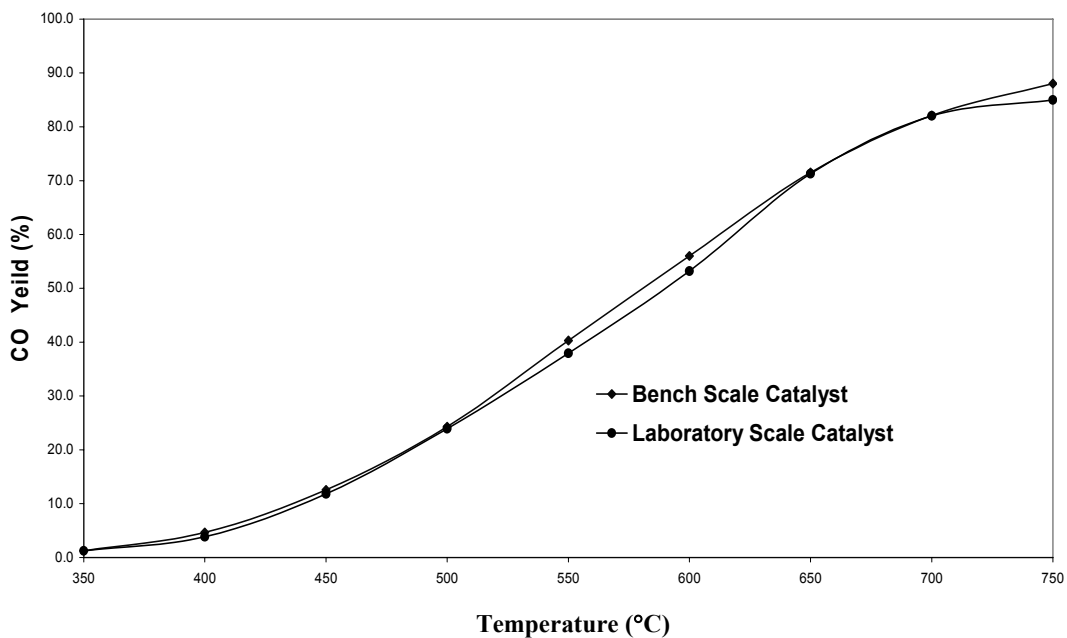

Figure 12. Comparison of CO yield in the dry reforming reaction using catalysts prepared at the laboratory- and bench-scales

Nomenclature

b	blade width (cm)
C_p	heat capacity (kJ/kg°C)
D_T	tank diameter (cm)
D_a	mixer diameter (cm)
h	convective heat transfer coefficient (W/m²°C)
H	liquid depth (cm)
ID	inside diameter (cm)
K	conductive heat transfer coefficient (J/m.K)
L	blade length (cm)
N	mixer rotation (rpm)
OD	outside diameter (cm)
Q_{loss}	thermal power lost (kW)
$Q_{latentheat}$	latent heat of vaporization (kW)
t	time (S)
Z	space between mixer and tank bottom (cm)
FI	Inertia force (N)
FV	Viscous force (N)
Fs	Surface tension force (N)

Greek letters

ρ	fluid ensity (Kg/m3)
λ	latent heat of vaporization (kW)
μ	viscosity (Pa.S)
μw	viscosity at wall temperature (Pa.S)
ΔT1	Temperature difference between initial and final solution. (°C)
ΔT1	Temperature difference between tank wall and solution. (°C)

Dimensionless numbers

Re	Reynolds number
Pr	Prandtl number
We	Weber number

References

1. Walas, S.M., Chemical Process Equipment, Butterworth-Heinmann Series in Chemical Engineering, USA, p. 287-303 (1990).

2. Havas, G., Deák, A. and Sawinsky, J., "The effect of the impeller diameter on the heat transfer in agitated vessels provided with vertical tube baffles" The Chemical Engineering Journal, 27 (3), 197 (1983).

3. Mohan, P., Emery, A.N. and Al-Hassan, T., "Review heat transfer to Newtonian fluids in mechanically agitated vessels", Experimental Thermal and Fluid Science, 5 (6), 861 (1992).

4. Delaplace, G., Demeyre, J. F., Guérin, R., Debreyne, P. and Leuliet, J. C., "Determination of representative and instantaneous process side heat transfer coefficients in agitated vessel using heat flux sensors", Chemical Engineering and Processing, 44 (3), 993 (2005).

5. Yaws, Carl L., Chemical Properties Handbook: physical, thermodynamic, environmental, McGraw-Hill, p. 30-83 (1999).

6. Groote, A.M.D., Froment, G.F., "The role of coke formation in catalytic partial oxidation for synthesis gas production", Catalysis Today, 37 (3), 309 (1997).

7. Rostrup-Nielsen, J.R., "New aspects of syngas production and use", Catalysis Today, 63 (2), 159 (2000).

8. Jones, R.H. Ashcroft, A.T., Waller, D., Cheetham, A.K. and Thomas, J.M., "Catalytic conversion of methane to synthesis gas over europium iridate, Eu2Ir2O7: Anin situ study by x-ray diffraction and mass spectrometry", Catalysis Letter, 8 (2), 169 (1991).

9. Ashcroft, A. T., Cheetham, A. K., Jones, R. H., Natarajan, S., Thomas, J. M., Waller, D., Clark, S. M., "An in situ, energy-dispersive x-ray diffraction study of natural gas conversion by carbon dioxide reforming", Journal of Physical Chemistry, 97 (13), 3355 (1993).

10. Khalesi, A., Arandiyan, H.R., Parvari, M., "Production of Syngas by CO2 reforming on MxLa1−xNi0.3Al0.7O3−d (M = Li, Na, K) catalysts", Industrial and Engineering chemistry Research, 47(16), 5892 (2008)

11. Bhattacharya, A.K., Breach, J.A., Chand, S., Ghorai, D.K., Hartridge, A., Keary, J., Mallick, K.K., "Selective oxidation of methane to carbon monoxide on supported palladium catalyst", Applied Catalysis A: General, 80 (1), L1-L5 (1992).

12. Hochmuth, J.K., "Catalytic partial oxidation of methane over a monolith supported catalyst", Applied Catalysis B: Environmental, 1(2), 89 (1992).

13. Hickman, D. A., Schmidt, L. D., "Steps in CH4 oxidation on Pt and Rh surfaces: High-temperature reactor simulations", AICHE Journal, 39 (7), 1164 (1993).

14. Otsuka, K., Ushiyama, T., Yamanaka, I., "Partial Oxidation of Methane Using the Redox of Cerium Oxide", Chemistry Letter, 22(9), 1517 (1993).

15. Dissanayake, D., Rosynek, M.P., Kharas, K.C., Lunsford, J.H., "Partial oxidation of methane to carbon monoxide and hydrogen over a Ni/Al2O3 catalyst", Journal of Catalysis, 132 (1), 117 (1991).

16. Ruckenstein, E., Hang Hu, Y., "Carbon dioxide reforming of methane over nickel/alkaline earth metal oxide catalysts", Applied Catalysis A: General, 133 (1), 149 (1995).

17. Kim, J.H., Suh, D.J., Park, T.J., Kim, K.L., "Effect of metal particle size on coking during CO2 reforming of CH4 over Ni–alumina aerogel catalysts", Applied Catalysis A: General, 197 (2), 191 (2000).

18. Suh, D.J. Park, T.J., Kim,J.H., Kim, K.L., "Nickel–alumina aerogel catalysts prepared by fast sol–gel synthesis", Journal of Non-Crystalline Solids, 225 (1), 168 (1998).

20. Parvary, M., Jazayeri, S. H., Taeb, A., Petit, C., Kiennemann, A., "Promotion of active nickel catalysts in methane dry reforming reaction by aluminum addition", Catalysis Communications, 2 (11), 357 (2001).